Structure of the breathing mode of the nucleon from high-energy p-p scattering

H. P. Morsch
Institut für Kernphysik, Forschungszentrum Jülich, D-52425 Jülich, Germany

P. Zupranski
Soltan Institute for Nuclear Studies, PL-00681 Warsaw, Poland

(Received 4 March 2004; revised manuscript received 15 February 2005; published 21 June 2005)

Spectra of p-p and π-p scattering at beam momenta between 6 and 30 GeV/c have been reanalyzed. These show strong excitation of N^* resonances, the strongest one corresponding to the "scalar" P_{11} excitation (breathing mode) at $m_0 = 1400 \pm 10$ MeV with $\Gamma = 200 \pm 20$ MeV. The result of a strong scalar excitation is supported by a large longitudinal amplitude $S_{1/2}$ extracted from e-p scattering. From exclusive data on $p + p \rightarrow pp\pi^+\pi^-$, a large 2π-N decay branch for the P_{11} resonance of $B_{2\pi} = 75 \pm 20\%$ has been extracted.

The differential cross sections were described in a double-folding approach, assuming multigluon exchange as the dominant part of the effective interaction between the constituents of projectile and target. First, the parameters of the interaction were fitted to elastic scattering; then, with this interaction, the inelastic cross sections were described in the distorted wave Born approximation (DWBA). A good description of the data requires a surface peaked transition density, quite different from that of a pure radial mode. In contrast, the electron scattering amplitude $S_{1/2}$ is quite well described by a breathing mode transition density with radial node. This large difference between charge and matter transition densities suggests that in p-p scattering the coupling to the multigluon field is much more important than the coupling to the valence quarks. A multigluon (or sea-quark) transition density is derived, which also shows breathing, indicating a rather complex multiquark structure of N and N^* including additional multigluon (or $q^{2n}\bar{q}^{2n}$) creation out of the ground state vacuum.

DOI: 10.1103/PhysRevC.71.065203 PACS number(s): 14.20.Gk, 13.75.−n, 13.85.−t, 25.40.−h

I. INTRODUCTION

The spectrum of baryon resonances is directly related to the dynamical structure of quantum chromodynamics; however, the origin of these resonances is not well understood. In particular, the lowest N^* resonance, P_{11} at a mass of about 1400 MeV (Roper resonance), has been discussed controversially in many different models, such as the constituent quark model [1,2], the Skyrmion model [3], and bag models [4], being of hybrid structure [5], or generated by a strong σ-N coupling [6]. Recent calculations in lattice QCD [7] have shown that the mass of the lowest P_{11} is reproduced in quenched approximation, indicating that this resonance contains seizable valence quark contributions.

Experimentally, the lowest P_{11} resonance exhibits a rather complex structure, which shows up differently in several reactions: whereas in π-N phase shift analyses [8] this resonance is quite weak and has a large width of the order of 350 MeV, in α-p scattering [9] a strong monopole excitation has been found in this mass region with a much smaller width of about 200 MeV. In inclusive electron scattering data [10] a P_{11} resonance has not been observed; however, in γ-induced processes it is rather small but clearly observed (see, e.g. [11]). In an attempt to understand the different results, a T-matrix description of α-p, π-N, and γ-p has been performed [12], which shows that all data can be described consistently by assuming two structures in this resonance, a strong scalar monopole excitation (Saturne resonance) interpreted as the breathing mode of the nucleon, and a second much wider structure, which can be interpreted as second order Δ excitation (spin-isospin ($M1$) mode). Preliminary results from a more exclusive study of α-$p \rightarrow \alpha'(p, \pi^+)x$ [13] support these conclusions.

To study further N^* resonances, we have analyzed old p-p and π-p scattering data [14–16] taken at beam momenta above 5 GeV/c, in which a pronounced resonance structure is observed. The analysis of these spectra is discussed in Sec. II with emphasis on the breathing mode excitation P_{11} at 1400 MeV. The decay properties of this resonance are discussed in Sec. III. Then an attempt is made in Secs. IV and V to understand the breathing mode excitation in p-p and e-p, which necessitates the assumption of a strong multigluon field in the nucleon. From this phenomenological analysis, new insight into the structure of scalar N^* excitations is obtained.

II. ANALYSIS OF p-p AND π-p SPECTRA

In the p-p and π-p spectra of Refs. [14–16], several resonance structures have been observed: the $\Delta(1232)$ and resonances at about 1400, 1520, 1680, and 2190 MeV. Remarkably, by far the strongest resonance (at small momentum transfer) is found in the region of the lowest P_{11}. It is important to mention that the wealth of p and π scattering data in this energy region, taken at very different momentum transfers, showed evidence just for these few resonances (in contrast to low energy π-N, in which many more resonances show up). This indicates a high selectivity in the excitation of N^* resonances (with quantum numbers $J^\pi = L \pm \frac{1}{2}^{(-)^L}$, where L is the angular momentum transfer). This can be explained by the fact that multigluon exchange (of scalar character) is the predominant part of the interaction (see, e.g., [17]).

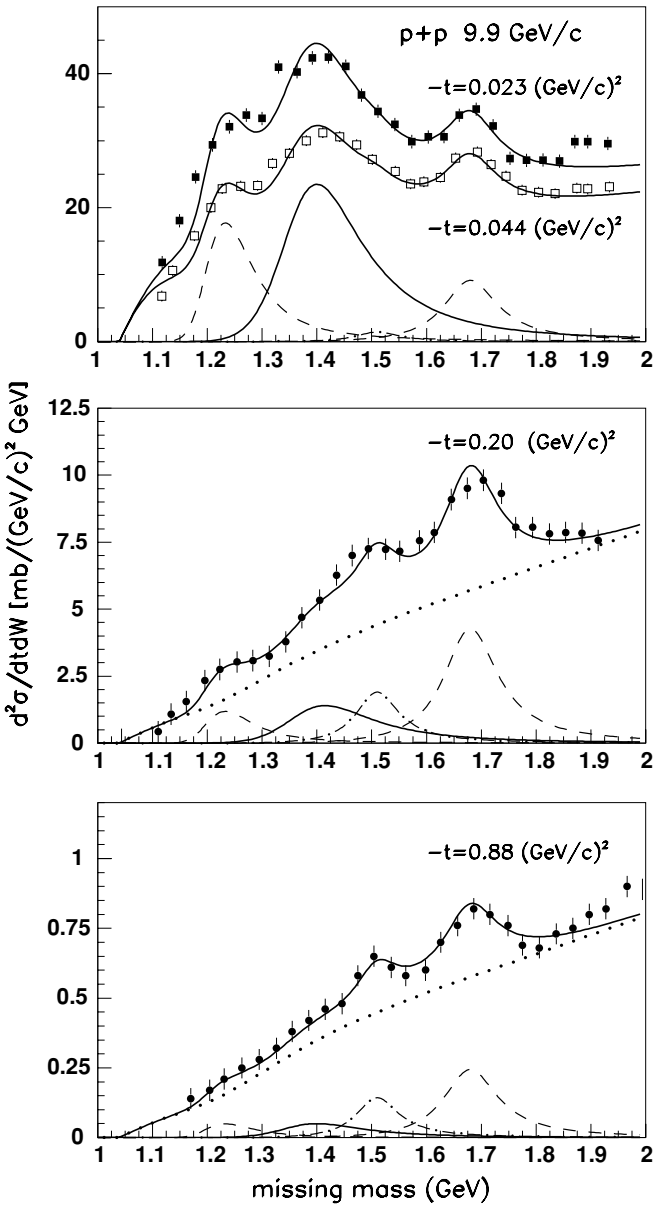

FIG. 1. Missing mass spectra for p-$p \to p' + x$ at a beam momentum of 9.9 GeV/c from Ref. [15] in comparison with resonance fits (solid lines) using a background shape (dotted lines) given by Eq. (1). The separate resonances are given; in particular, strong excitation of the P_{11} at 1400 MeV at small momentum transfer is indicated by solid lines.

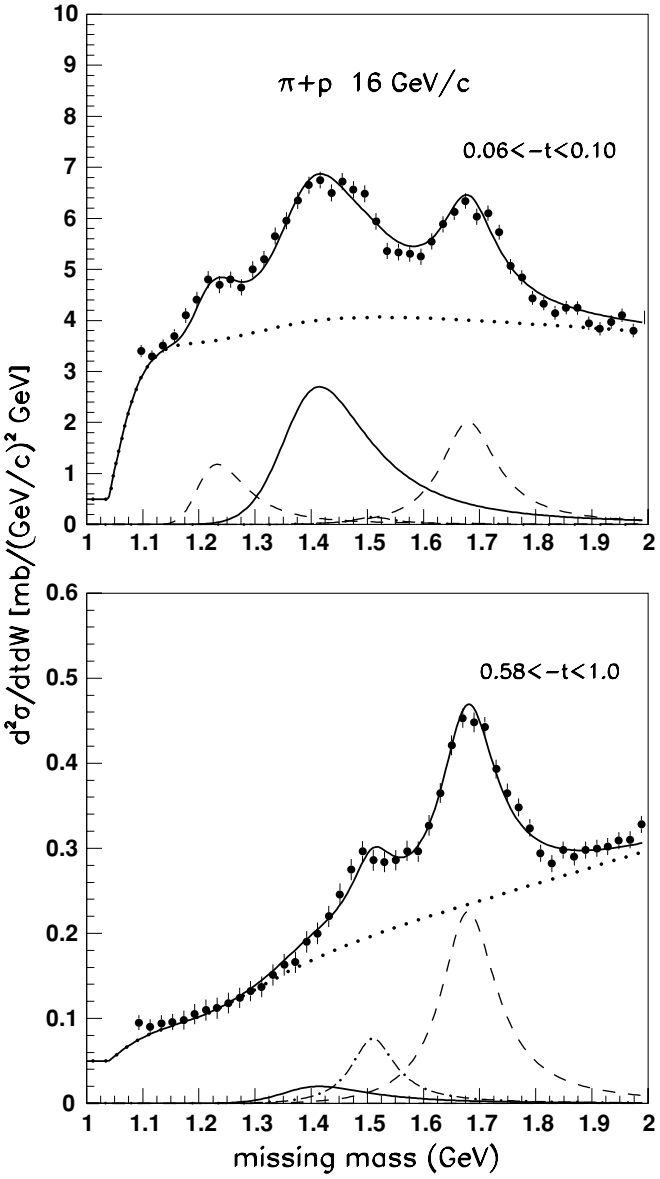

FIG. 2. Missing mass spectra for $\pi - p \to \pi' + x$ at a beam momentum of 16 GeV/c from Ref. [15] in comparison with resonance and background fits similar to those in Fig. 1.

Missing mass spectra of p-p and π-p scattering are shown in Figs. 1–4 together with resonance fits given by solid lines. Apart from the P_{11}, the shapes were taken from a fit of π-N phase shift amplitudes (see Refs. [12,17]), using modified Breit-Wigner forms. A multipion background is also important, which is described by 1π and 2π threshold functions of a form similar to that used in Ref. [12], together with a polynomial rise to larger masses,

$$\text{back}(m) = \sum_{n=1}^{2} [c_n f_{n\pi} + d_n (m - m_{n\pi})^n], \qquad (1)$$

with $f_{n\pi} = [(\beta - 1)/(\beta + 1)]^n$ and $\beta = \exp[\frac{(m - m_{n\pi})}{(m_0 - m_{n\pi})} C_{n\pi}]$. A value of m_0 of 1.35 GeV is needed, when strong Δ excitation is observed (at low beam momentum $\leqslant$10 GeV/c and small momentum transfer $\leqslant$0.05 (GeV/c)^2); otherwise m_0 is about 1.48 GeV (or 1.55 at $-t \leqslant 0.2$ (GeV/c)^2). For $C_{1\pi}$ and $C_{2\pi}$, values of 15 and 4 were used. We fitted the background in all p-p spectra from 6 to 20 GeV/c simultaneously with a smooth variation of the parameters c_n and d_n ($c_1 \sim$(5-10)c_2, $d_1 \sim 1/3 c_2$, and d_2 very small). For a small momentum transfer of $t = 0.044$ (GeV/c)^2 the threshold parameter c_1 falls off towards higher beam momenta by a factor of two, whereas d_1 decreases by about a factor of four. As a function of momentum transfer, the threshold term drops rather fast, whereas the linear term falls off much less. The quadratic term (with amplitude d_2) was negligible at smaller momentum transfers and still

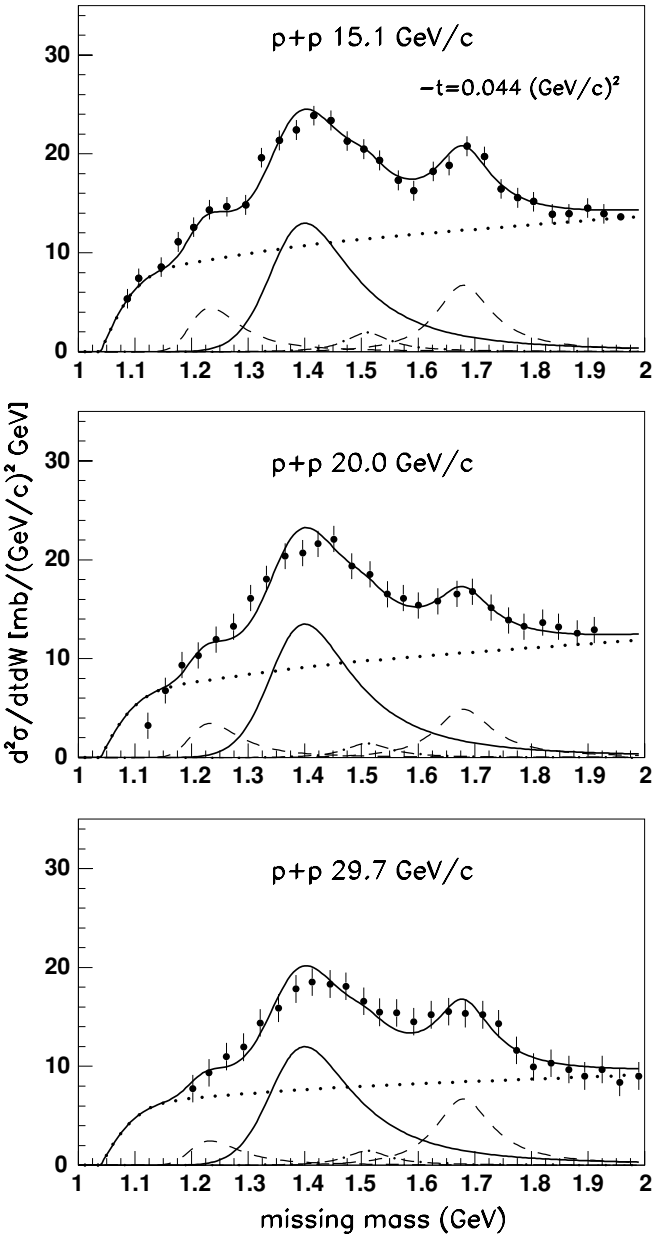

FIG. 3. Missing mass spectra for p-$p \rightarrow p' + x$ at beam momenta of 15.1, 20.0, and 29.7 GeV/c at a momentum transfer of 0.044 (GeV/c)^2 from Ref. [15] in comparison with resonance and background fits similar to those in Fig. 1.

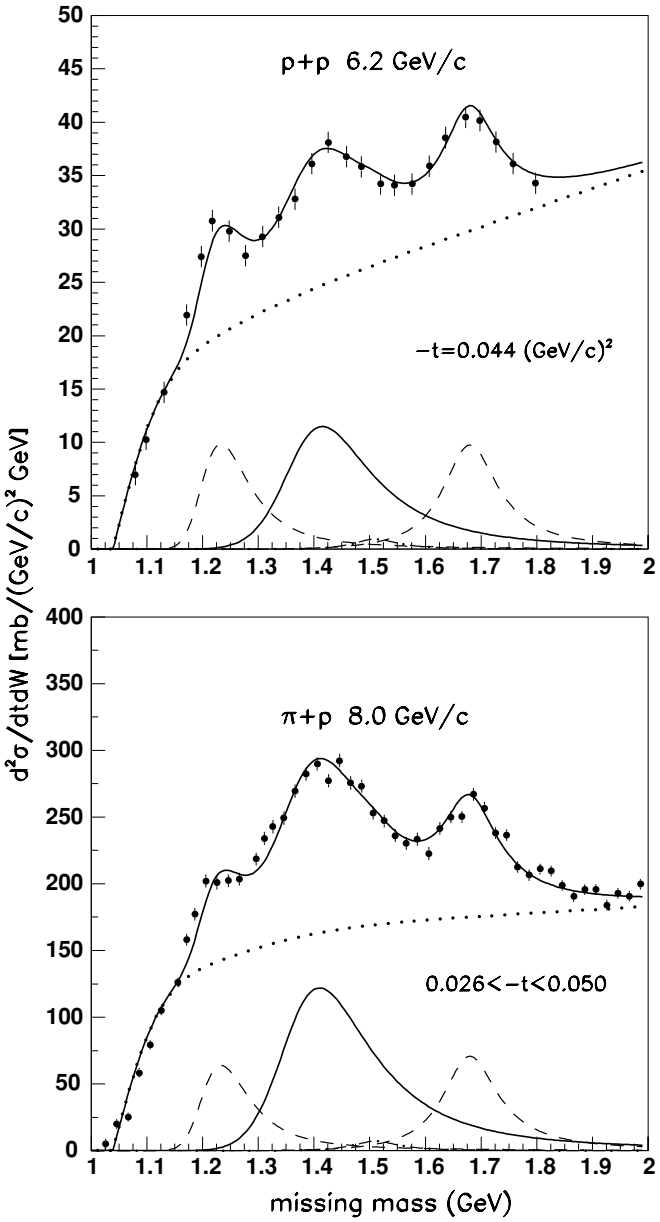

FIG. 4. Missing mass spectra for p-$p \rightarrow p' + x$ at a beam momentum of 6.2 GeV/c (upper part) and $\pi - p \rightarrow \pi' + x$ at a beam momentum of 8.0 GeV/c from Refs. [15,16] in comparison with resonance and background fits similar to those in Fig. 1.

quite small at values of $-t > 0.6\,\mathrm{GeV}/c^2$. As already discussed in former work (see, e.g., [15]), the background fits give rise to uncertainties in the absolute resonance cross sections up to 30%. However, the positions and widths of the resonances are not much affected. Examples of the p-p and π-p fits at different momentum transfers are given in Figs. 1 and 2.

In fitting the spectra, we used the $\Delta_{33}(1232)$, the known N^* resonances $D_{13}(1520)$ and $F_{15}(1680)$, and strong excitation of a resonance at 1400 MeV [14–16]. In the former studies (see, e.g., [14]) it has already been questioned whether this structure at 1400 MeV could be the Roper resonance $P_{11}(1440)$ observed in π-N, because this peak is not exactly at the position of this resonance (masses of resonances were determined precisely in the spectrometer experiments [14,15]). Other possibilities have been discussed (e.g., special kinematic effects), but these are not likely to explain the strongest resonance observed (which is stronger than the $\Delta(1232)$ excitation). Remarkably, at higher energies this resonance corresponds in mass and width closely to the Saturne resonance observed in α-p scattering [9] (see Table 1). Using all data above 9 GeV/c, we obtain a centroid mass of the P_{11} resonance of 1400 ± 10 MeV with a width of 200 ± 20 MeV (this is better determined than from α-p, which has a strong form factor dependence). Further, the cross section of this resonance is peaked strongly at small

TABLE I. Deduced resonance parameters of the P_{11} resonance.

Reaction	Beam momentum GeV/c	m_0	Γ
α-p	7	1390 ± 20	190 ± 30
p-p	10-30	1400 ± 10	200 ± 20
π-p	16	1400 ± 15	200 ± 25
p-p	6.2	1415 ± 10	205 ± 20
π-p	8	1410 ± 15	200 ± 25
π-N	low E (Ref. [8])	1440 ± 30	360 ± 80
γ-N	low E (Ref. [11])	1463 ± 10	360 ± 20

momentum transfers, characteristic of $L = 0$ excitation (see Fig. 1).

As discussed in Sec. I, evidence for two structures has been obtained [12]: one in the region of the lowest P_{11} (Roper resonance), the breathing mode which is strongly excited in high energy p-p, and a second mode related to the Δ degree of freedom. In the lower energy p-p data at about 6 GeV/c and π-p at 8 GeV/c (Fig. 4), we observe still a rather strong excitation of the $\Delta(1232)$, which decreases towards higher proton momenta. This is indicative of π exchange, which should allow small excitation of the second structure. Indeed, in the spectra shown in Fig. 4 the P_{11} peak is somewhat shifted to a higher mass (see Table I), which may be due to the effect of the second P_{11} structure.

Results on the longitudinal e-p amplitude $S_{1/2}$ yield complementary information on scalar N^* excitations. Different from hadron scattering, longitudinal electron scattering becomes very small at higher energies. In the inclusive $p(e, e')$ data from SLAC [10], the $\Delta(1232)$ and N^* resonances at 1520 and 1680 MeV have been observed, but the P_{11} is missing. This can be taken as evidence that the latter resonance has only a small transverse component at large momentum transfers.

From recent exclusive e-p scattering experiments at JLab using a polarized electron beam, the longitudinal amplitude $S_{1/2}$ of the P_{11} excitation could be extracted [18]. This amplitude is rather large, supporting our findings of an important breathing mode excitation.

III. DECAY OF THE P_{11} AT 1400 MEV FROM EXCLUSIVE DATA

Information on the decay of the strong P_{11} resonance can also be deduced from high-energy experiments. At a beam momentum of 6.6 GeV/c four-prong events have been studied [19] in p-p scattering, which are related to $p + p \rightarrow pp\pi^+\pi^-$. In the invariant $\pi^+\pi^-$ mass spectrum (Ref. [19], Fig. 7a), a strong rise of the yield has been observed above the $2\pi N$ threshold (see Fig. 5), which is very different from phase space. We calculated the $\pi^+\pi^-$ mass spectrum corresponding to the resonances observed in Figs. 1–4 and found that, indeed, the resonance at 1400 MeV gives rise to a strong peak in the $\pi^+\pi^-$ spectrum, whereas the resonances at higher masses are smeared out. This suggests strong 2π-N decay of this resonance.

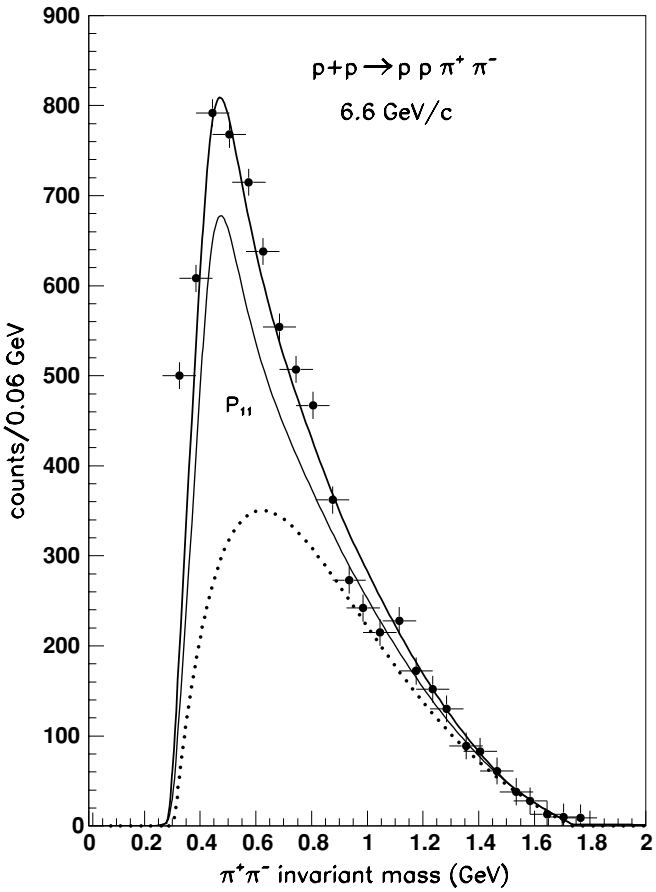

FIG. 5. Invariant $\pi^+\pi^-$ mass spectrum from the data in Ref. [19] in comparison with a resonance fit (upper solid line) consistent with Fig. 1. The 2π background without and with the contribution of the P_{11} at 1400 MeV is given by the dotted and lower solid line, respectively.

To calculate the complete 2π spectrum, a background has been computed (dotted line) using a form consistent with that in Eq. (1) multiplied by the 2π phase space. As shown by the upper solid line in Fig. 5, a reasonable description of the spectrum is obtained. Indeed, the strongest resonance contribution is due to the P_{11}, but the higher resonances $D_{13}(1520)$ and $F_{15}(1680)$ are needed also. The latter contributions are on the order of 40% of that of the P_{11} at 1400 MeV with a somewhat larger yield from the $F_{15}(1680)$. The $D_{13}(1520)$ and $F_{15}(1680)$ decay mainly into the $1\pi N$ channel [8] with a branching ratio of about 60 and 70%, respectively. These resonances are clearly observed in the two-prong events of the p-p scattering data [20], whereas no clear signal of $1\pi N$ decay is observed for the resonance at 1400 MeV.

In order to estimate the 2π decay branch of the P_{11} resonance, we have to take into account the fact that the spectrum in Fig. 5 is integrated over momentum transfer. In the low momentum transfer spectra in Fig. 1, the ratio of P_{11} to F_{15} cross sections is about 3; integrating over all momentum

transfers[1] up to 1.2 (GeV/c)^2, we obtain about equal yields (for larger values of $-t$ the contributions are small). From this, we extract a $2\pi N$ branch of the P_{11} of $75 \pm 20\%$. This is consistent with the result in Ref. [12] ($\sim$80%). Further, this supports former explanations of the 1400 MeV resonance (see Ref. [14]), being a highly inelastic resonance in π-N, which decays only weakly into the elastic channel.

IV. DESCRIPTION OF THE p-p DIFFERENTIAL CROSS SECTIONS

To understand the differential cross sections, we performed calculations within the framework of the distorted wave Born approximation (DWBA) similar to those in Ref. [17], assuming multigluon exchange of scalar structure as the predominant part of the effective interaction. First, elastic scattering was described by a double-folding potential similar to that in Ref. [17]. By fitting the experimental data, the strength of the effective interaction and the nucleon radius were determined. We obtained results which represent an excellent extrapolation of the potential strengths and mean square radii deduced at lower energies (See Ref. [17], Figs. 6 and 7). For a proton momentum of 15.1 GeV/c, results are given in Fig. 6 using volume integrals of the central real and imaginary potential I_V and I_W of about 520 and 640 MeV fm^3, respectively, and a nucleon mean square radius $\langle r^2\rangle_N$ of about 0.45 fm^2. At proton energies above 1 GeV, the Lorentz boost gives rise to a contraction of the projectile in the beam direction, leading to smaller values of $\langle r^2\rangle_N$. On the other hand, the systematics of p-p scattering at high energies shows the opposite effect, increasing slope parameters toward higher energies [21], which may point to larger interaction radii. This may be understood by an increase of multiple scattering. Our result of $\langle r^2\rangle_N = 0.45$ fm^2, as compared to 0.66 fm^2 at smaller energies, is well described by the boost effect, indicating that at the energies in question, multiple scattering is still rather small.

With these potentials inelastic (p, p') cross sections for resonance excitation were calculated in DWBA. The details of these calculations are similar to those in Ref. [17]. As a result, the t dependence of the calculated cross section shows a diffraction pattern only for $L = 0$ transfer, with a slope as oberved for the resonance at 1400 MeV. This is because the same partial waves contribute to the initial and final state wave functions. Thus, our calculations confirm quite model-independently a P_{11} assignment of this resonance. For larger L transfers, the diffraction pattern is washed out due to the contribution of different partial waves in the overlap of initial and final state wave functions. This is observed for the $L = 2$ excitation of the $F_{15}(1680)$, where the momentum transfer dependence is rather flat. Here we want to mention that the basic features of our DWBA approach are quite consistent with the former theoretical approach in Ref. [22] that gave only a very qualitative account of the N^* yields.

[1]For this integration we used the differential cross sections calculated in the DWBA (see Sec. IV).

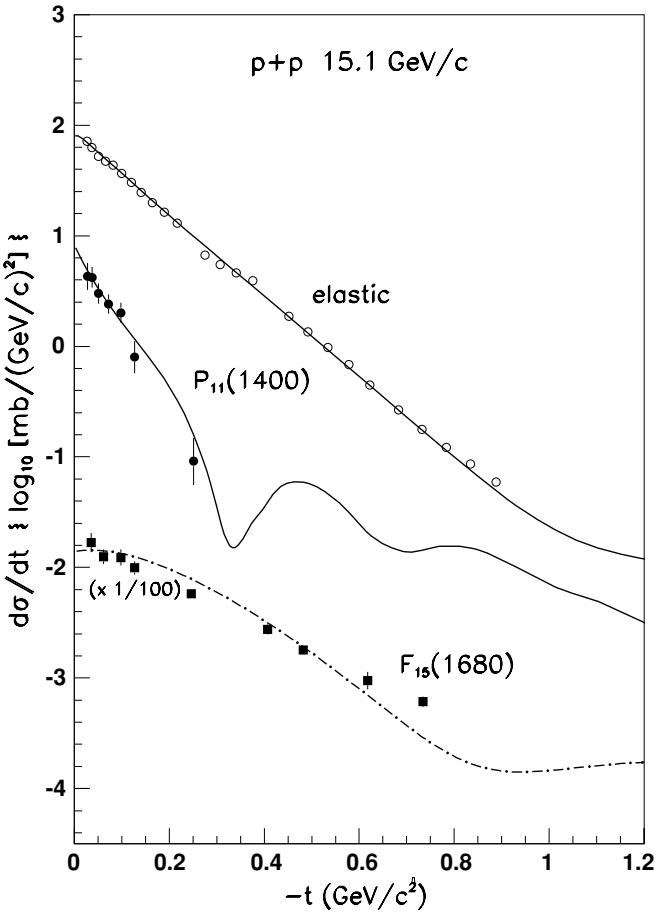

FIG. 6. Differential cross sections for elastic scattering and inelastic excitation of resonances at 1400 and 1680 MeV for 15.1 GeV/c p-p scattering from Ref. [15] together with the result of our DWBA calculations.

It is important to note that the calculated t dependence of the differential cross section is sensitive to details of the transition density. By using different forms, we found that the experimental cross sections in Fig. 6 can by described only by a surface peaked transition density (quite similar to that in Ref. [17], Fig. 10, dashed line). In Sec. V, an attempt is made to understand this transition density together with the data from e-p scattering. The absolute cross section of the breathing mode excitation is reproduced with a monopole strength covering a significant fraction of the full energy weighted sum rule strength [17,23], in good agreement with the results of α-p.

V. HOW CAN WE UNDERSTAND THE BREATHING MODE EXCITATION IN p-p AND e-p?

The dominance of multigluon exchange [17] in p-p scattering at the energies in question can be taken as an indication that this reaction probes to a large extent the multigluon structure of the nucleon (in addition to some valence quark excitation). Support for strong multigluon contributions to the breathing mode excitation is also obtained from the deduced hadron

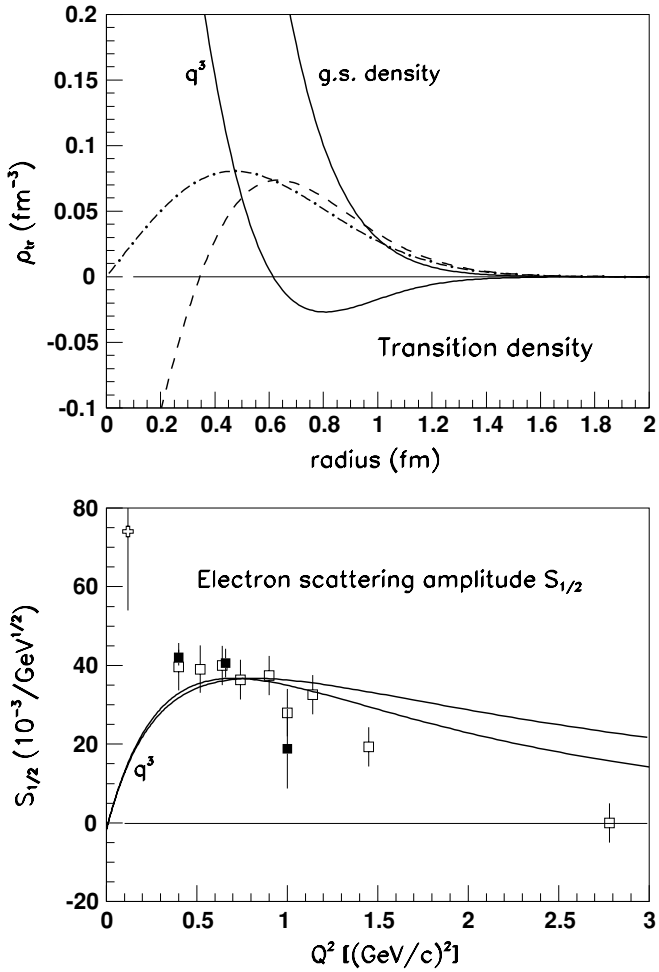

FIG. 7. Transition densities derived from p-p and e-p data (upper part) and longitudinal e-p scattering amplitude $S_{1/2}$ with the data from Ref. [18] (lower part). The solid lines (apart from the g.s. density) describe $S_{1/2}$, whereas the dot-dashed line results from a fit of p-p. The dashed line indicates the sea quark contributions arising from the multigluon field.

compressibilities [23], which were found to be flavor and isospin independent, and thus quite likely associated with the multigluon field of hadrons. Such gluonic contributions are also expected from the basic structure of QCD, which involves strong self-interactions of gluons.

In the breathing mode excitation, a large fraction of the energy weighted sum rule strength is observed; this allows us to approximate the transition density $\Delta\rho_o(r)$ in a fluid-dynamical picture by dynamical distortions of the ground state (g.s) density $\rho(r)$ with respect to the central density ρ_o and the density falloff m. Using for this a form $\rho(r) = \rho_0 \exp(-mr^\kappa)$ (with values of κ between 1 and 2) gives

$$\Delta\rho_0(\vec{r}) = \left[\delta\rho_0 \frac{\partial\rho(r)}{\partial\rho_0} f_0(r) + \delta m \frac{\partial\rho(r)}{\partial m} + (h.o.)\right] Y_0(\theta,\phi). \tag{2}$$

The amplitudes $\delta\rho_0$ and δm were varied to obtain a reasonable fit of the differential cross sections; furthermore, $f_0(r) = 1$ was used.

A good description of the p-p differential cross sections in Fig. 6 is obtained asssuming only a distortion $\delta m \neq 0$ of the surface term. This is very different from our expectation for a radial excitation mode (see [17]) with the constraint $\int \Delta\rho_0(r) r^2 dr = 0$, for which $\delta\rho_0$ and $\delta m \neq 0$. To be able to compare the extracted transition density with e-p scattering, boost effects should be removed. For this, the resulting transition density was revalued for a density yielding $\langle r^2\rangle_N = 0.66$ fm^2, given by the dot-dashed line in the upper part of Fig. 7.

As pointed out, the longitudinal e-p amplitude $S_{1/2}$ [18] yields complementary information on the breathing mode excitation. The charge transition density was assumed of the same form as Eq. (2), using a charge density consistent with Ref. [24] and the additional constraint $\int \Delta\rho_{\rm ch}(r) r^2 dr = 0$ (charge conservation), which requires $\delta\rho_0$ and $\delta m \neq 0$. A fit of the experimental data is given in the lower part of Fig. 7 with a transition density as given by the solid line in the upper part. The transformation of the transition density to a Q^2 dependence was made according to Ref. [24] (the two lines are for $\lambda = 1$ and 2 and may indicate the size of uncertainties in the relativistic transformation). Because for the valence quarks (q^3) $\int \Delta\rho_{q^3}(r) r^2 dr = 0$ also, the charge transition density corresponds essentially to that of the valence quarks. Our results are consistent with lattice QCD calculations [7] indicating a seizable valence quark excitation in the low-lying P_{11} resonance. Actually, from recent lattice calculations [25], information on the radial wave functions of the nucleon ground and first excited state could be extracted. These show a node in the P_{11} wave function, supporting the breathing mode picture.

The deduced transition density of the valence quarks, $\Delta\rho_{q^3}(r) \approx \Delta\rho_{\rm ch}(r)$ (solid line in Fig. 7, upper part) is very different from the matter (multigluon plus q^3) transition density derived from p-p (dot-dashed line). This suggests strongly that in p-p the relative q^3 coupling R_{q^3} (with respect to the coupling to the multigluon field) is rather small. Assuming for R_{q^3} a value of 0.3, the multigluon (or sea quark) part of the transition density is given by the dashed line. This component is almost an order of magnitude stronger than the valence quark component in p-p, and with opposite phase. Further, it also shows "breathing" (node in the transition density), indicating that strong sea quark components due to the multigluon field are already present in the g.s. density (again confirming our assumption of a strong multigluon field). Qualitatively similar results are obtained for even smaller values of R_{q^3} (which are probably more realistic). Further, the surface peaked matter transition density (dot-dashed line) indicates in addition creation of multiglue (or $q^{2n}\bar{q}^{2n}$) components out of the g.s. vacuum.

VI. SUMMARY

The present analysis of high-energy p-p scattering data has confirmed our evidence for a "scalar" P_{11} excitation, which covers the full energy weighted sum rule (breathing mode). The properties of this remarkable excitation ($L = 0$ *without spin-isospin flip, mass* ~1400 MeV, *width* ~200 MeV, *dominant* 2π-N *decay*) are quite different from those of the P_{11} resonance observed in low-energy π-N

and γ-N (*dominant* $L = 0$ *spin-isospin* ($M1$) *excitation, mass* $\sim$ 1440 MeV, *width about* 360 MeV, *dominant* 1π-N *decay*); this supports strongly the two resonance picture of the lowest P_{11} (Roper) resonance. In the low-energy reactions π-N and γ-N the breathing mode has not been detected. For π-N, this can be understood by the fact that the S-wave interaction is strongly reduced as compared to P-wave excitation; in addition, the coupling to π-N is further suppressed due to the dominant $2\pi N$ branch of this resonance. In the case of γ-induced reactions, a pure scalar $L = 0$ state cannot be excited. However, both in π-N, and γ-N, strong coupling to the Δ degree of freedom is observed, which allows excitation of the second P_{11} structure understood as Δ excitation of the $\Delta(1232)$.

The evidence for the breathing mode is further supported by recent polarized e-p scattering data, from which the longitudinal amplitude $S_{1/2}$ has been extracted. An attempt has been made to understand the data on p-p and e-p consistently. For this, it was necessary to assume the existence of strong multigluon contributions in the nucleon density consistent with the vacuum structure of Yang-Mills theory. In longitudinal electron scattering, only charge contributions (mainly valence quarks) are seen, whereas the interaction in p-p probes mainly the multigluon structure (giving rise to strong sea quark contributions). This yields evidence for a rather complex multiquark structure of baryons.

Future experimental work should provide more details on the interplay of quark and gluonic structure. This is possible in detailed studies of selective hadronic and electromagnetic reactions, as discussed in the present paper. Therefore, complementary to the large efforts made at Jlab with polarized electron scattering experiments, selective N^* excitation in p-α scattering with clear separation of the important $2\pi N$ decay channels—$2\pi(s)$-N, $2\pi(p)$-N, and π-Δ—and other channels are planned at the COSY p-beam facility.

ACKNOWLEDGMENT

We thank Piotr Decowski for many comments and suggestions.

[1] N. Isgur and G. Karl, Phys. Rev. D **18**, 4187 (1978); S. Capstick and N. Isgur, *ibid.* **34**, 2809 (1986).
[2] L. Y. Glozman and D. O. Riska, Phys. Rep. **268**, 263 (1996).
[3] C. Hajduk and B. Schwesinger, Phys. Lett. **B140**, 172 (1984); B. Schwesinger, Nucl. Phys. **A537**, 253 (1992).
[4] P. J. Mulders, G. Bhamathi, L. Heller, A. T. Aerts, and A. K. Kerman, Phys. Rev. D **27**, 2708 (1983); P. A. M. Guichon, Phys. Lett. **B164**, 361 (1985).
[5] T. Barnes and F. E. Close, Phys. Lett. **B125**, 89 (1983); Z. P. Li, V. Burkert, and Z. Li, Phys. Rev. D **46**, 70 (1992).
[6] O. Krehl, C. Hanhart, S. Krewald, and J. Speth, Phys. Rev. C **62**, 025207 (2000).
[7] W. Melnitchouk, S. Bilson-Thompson, F. D. R. Bonnet, J. N. Heddith, F. X. Lee, D. B. Leinweber, A. G. Williams, J. M. Zanotti, and J. B. Zhang, Phys. Rev. D **67**, 114506 (2003); N. Mathur *et al.*, Phys. Lett. **B605**, 137 (2005) and references therein.
[8] R. A. Arndt, I. I. Strakovsky, R. L. Workman, and M. M. Pavan, Phys. Rev. C **52**, 2120 (1995) and references therein.
[9] H. P. Morsch *et al.*, Phys. Rev. Lett. **69**, 1336 (1992).
[10] E. D. Bloom *et al.*, Phys. Rev. Lett. **23**, 930 (1969); F. W. Brasse *et al.*, Nucl. Phys. **B110**, 413 (1976) and references therein.
[11] R. A. Arndt, R. L. Workman, Z. Li, and C. D. Roper, Phys. Rev. C **42**, 1853 (1990); R. A. Arndt, I. I. Strakovsky, and R. I. Workman, *ibid.* **53**, 430 (1996); M. Wolf *et al.*, Eur. Phys. J. A **9**, 5 (2000).
[12] H. P. Morsch and P. Zupranski, Phys. Rev. C **61**, 024002 (1999).
[13] G. D. Alkhazov *et al.*, in *Proceedings of the COSY Workshop on "Baryon Excitations," Juelich, 2000*, edited by T. Barnes and H. P. Morsch, Schriften des Forschungszentrums Juelich, Vol. 6, 53 (2000); and to be published.
[14] E. W. Anderson *et al.*, Phys. Rev. Lett. **16**, 855 (1966).
[15] R. M. Edelstein *et al.*, Phys. Rev. D **5**, 1073 (1972) and references therein.
[16] E. W. Anderson *et al.*, Phys. Rev. Lett. **25**, 699 (1970).
[17] H. P. Morsch, W. Spang, and P. Decowski, Phys. Rev. C **67**, 064001 (2003).
[18] I. G. Aznauryan, V. D. Burkert, H. Egiyan, K. Joo, R. Minehart, and L. C. Smith, Phys. Rev. C **71**, 015201 (2005); (closed points in Fig. 7); L. Tiator *et al.*, Eur. Phys. J. **19**, 55 (2004) (open points in Fig. 7).
[19] E. Colton, P. E. Schlein, E. Gellert, and G. A. Smith, Phys. Rev. D **3**, 1063 (1971).
[20] E. Colton, Z. Ming Ma, G. A. Smith, and P. E. Schlein, Phys. Rev. D **7**, 3267 (1973).
[21] J. P. Burq *et al.*, Nucl. Phys. **B217**, 285 (1983).
[22] A. W. Hendry and J. S. Trefil, Phys. Rev. **184**, 1680 (1969).
[23] H. P. Morsch, Z. Phys. A **350**, 61 (1994).
[24] J. J. Kelly, Phys. Rev. C **66**, 065203 (2002); and references therein.
[25] Y. Chen, S. J. Dong, T. Draper, I. Horváth, F. X. Lee, K. F. Liu, N. Mathur, and J. B. Zhang (private communication).